Design and Performance of SuperSpec: An On-Chip, KID-Based, mm-Wavelength Spectrometer

E. Shirokoff · P. S. Barry · C. M. Bradford · G. Chattopadhyay · P. Day · S. Doyle · S. Hailey-Dunsheath · M. I. Hollister · A. Kovács · H. G. Leduc · C. M. McKenney · P. Mauskopf · H. T. Nguyen · R. O'Brient · S. Padin · T. J. Reck · L. J. Swenson · C. E. Tucker · J. Zmuidzinas

Abstract SuperSpec is an ultra-compact spectrometer-on-a-chip for mm and submm wavelength astronomy. Its very small size, wide spectral bandwidth, and highly multiplexed detector readout will enable construction of powerful multi-object spectrometers for observations of galaxies at high redshift. SuperSpec is a filter bank with planar, lithographed, superconducting transmission line resonator filters and lumped-element kinetic inductance detectors made from Titanium Nitride. We have built an 81 detector prototype that operates in the 195–310 GHz band. The prototype has a wide-band metal feed horn with a transition to microstrip that feeds the filter bank. The prototype has demonstrated optical filter bank channels with a range of resolving powers from 300 to 700, measured fractional frequency noise of 10^{-17}Hz^{-1} at 1 Hz.

Keywords Kinetic inductance detectors · Resonators · Millimeter-wavelength · Spectroscopy

E. Shirokoff (✉) · S. Hailey-Dunsheath · M. I. Hollister · A. Kovács · C. M. McKenney · S. Padin · J. Zmuidzinas · R. O'Brient
California Institute of Technology, Pasadena, CA, USA
e-mail: erik.shirokoff@caltech.edu

P. S. Barry · S. Doyle · P. Mauskopf · C. E. Tucker
School of Physics and Astronomy, Cardiff University, Cardiff, Wales, UK

C. M. Bradford · P. Day · H. G. Leduc · H. T. Nguyen · T. J. Reck ·
L. J. Swenson · J. Zmuidzinas · G. Chattopadhyay · R. O'Brient
Jet Propulsion Laboratory, Pasadena, CA, USA

P. Mauskopf
Arizona State University, Tempe, AZ, USA

1 Introduction

SuperSpec is an ultra-compact, wide-band spectrometer-on-a-chip for mm and submm wavelength astronomy [1,2]. The kinetic inductance detector (KID)-based design outlined here and in the accompanying paper[1] is a specific example of the filter-bank spectrometer circuit discussed in Kovács et al. [3]. The basic design is similar to other filter-bank spectrometers which appear in the literature by Tauber and Erickson [4], Galbraith et al. [5], Galbraith [6] and the contemporary project DESHIMA [7,8]. The tomographic ionized-carbon mapping experiment (TIME) project is testing devices which use a similar microstrip filter bank coupled to transition edge sensor (TES) bolometers.[2]

In this design, mm-wave radiation propagates along a feedline and past a series of half-wavelength transmission line mm-wave resonators. Each resonator is coupled to the feedline and to a power-detector, and thus functions as a tuned filter. The resonator frequencies are arranged monotonically and physically spaced quarter-wavelength from neighboring channels to minimize interaction between resonators.

The response of an individual filter channel at frequency f_i can be modeled as a shunt resonator. Its resolving power is given by $\mathscr{R} = f_i/\Delta f_i = 1/Q_{\text{feed}} + 1/Q_{\text{det}} + 1/Q_{\text{loss}}$, where the three Qs correspond to the coupling to the feedline, the power per cycle deposited in the detector, and the power per cycle which is absorbed elsewhere in the surrounding environment (e.g., $(\tan\delta)^{-1}$).

For efficient absorption, $Q_{\text{feed}} = Q_{\text{det}}$. The full spectrometer is created by arranging channels in a geometric progression, with a ratio of channel resolution to channel spacing determined by an adjustable oversampling factor Σ. As Σ increases, the total filter bank absorption efficiency can be larger than the 50 % maximum absorption in a single channel. A proposed 500 channel, $\mathscr{R} = 500$ SuperSpec demonstration instrument covering the 195–310 GHz band has $\Sigma = 2.1$ and greater than 80 % total absorption in band.

2 SuperSpec Prototype Design

The implementation of this filter bank design for the first generation SuperSpec prototype is shown in Fig. 1. The feedline and filter bank resonators are made from inverted microstrip consisting of 1 μm wide Nb traces on bare Si substrate, a 0.5 μm thick silicon nitride (Si_3N_x) dielectric deposited by plasma enhanced chemical vapor deposition and a Nb ground plane. The detectors are lumped-element KID (LEKIDs) made from 20 nm thick titanium nitride (TiN), with a transition temperature of approximately 2K [9,10]. The half-wavelength mm-wave resonator is proximity-coupled to both the feedline and to the meandered inductive portion of the KID. The coupling strengths can be independently tuned by adjusting the width of the gap between features.

The KID inductor is connected to an interdigitated capacitor (IDC) made from the same TiN layer deposited directly on the Si substrate. The ground plane and dielectric

---

[1] Hailey-Dunsheath et al., JLTP, submitted.
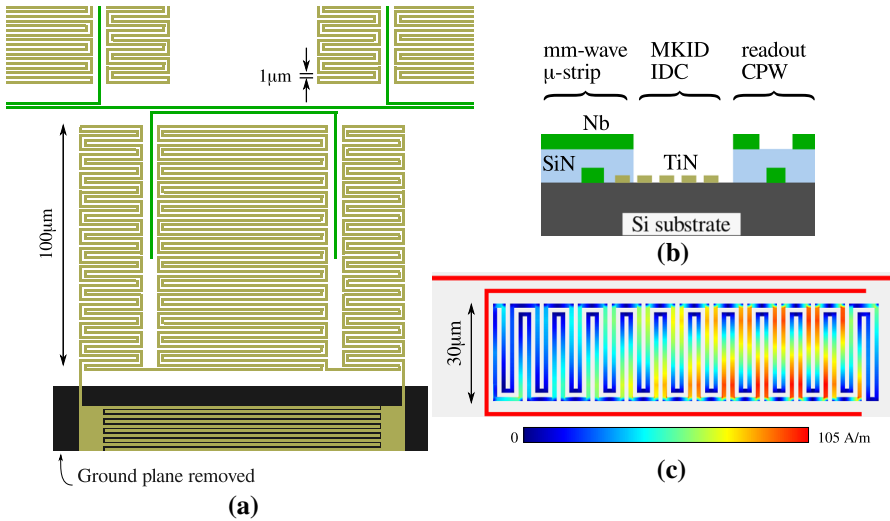
[2] Staniszewski et al., JLTP, submitted.

Fig. 1 **a** SuperSpec device detail, showing one full mm-wave resonator (*green* U-shaped structure), feedline, and the inductor and *top* portion of KID capacitor for one channel. **b** Cross section showing layers used in **a**. A thin SiO$_2$ layer for etch selectivity between the TiN and SiN layer is not shown. **c** Simulation of the new design (see Sect. 4), showing time-averaged current distribution at a single optical frequency. *Solid-red* currents in Nb microstrip are off-scale (Color figure online)

layer are removed in the region surrounding the capacitor to minimize the presence of two-level systems (TLSs) in regions of high electric field. The microwave readout line consists of 50 Ohm, bridged Nb CPW. The 7 μm wide center conductor is made from same layer as the Nb microstrip features. A small IDC couples each KID to the feedline, and its value determines the KID coupling-Q. The capacitance between the KID inductor and the ground plane dominates the current return path, but makes a negligible contribution to dissipation and TLS noise.

Both the mm-wave circuit and KID resonator were designed using the commercial, 3D planar method-of-moments solver Sonnet. The finite thickness of the Nb film increases the coupling by 50 % compared to thin film values at these dimensions. Sonnet's multi-sheet thick metal model was used to correct for thickness effects, after verifying that such a models agreed with ANSYS HFSS simulations of simplified mm-wave resonators.

The first generation prototype die includes 73 filtered channels, arranged in a sparse array from 180–270 GHz. These are arranged in several five-channel filter-banks and many isolated channels, some with intentionally mismatched Q_{feed} and Q_{det} designed to test simulation results. In addition to the filtered channels, the prototype includes eight broad-band detectors, for a total of 81 KIDs. Four of these broad-band detectors are identical to the filtered detectors, except that they are proximity coupled directly to the feedline and spatially distributed among the filtered channels. The remaining four broad band detectors are incorporated into a terminator that consists of several centimeters of meandering feedline surrounded by closely spaced TiN.

Incident radiation couples to a multiple-flare-angle smooth-walled horn [11]. The circular waveguide output from the horn transitions into single mode oval waveguide
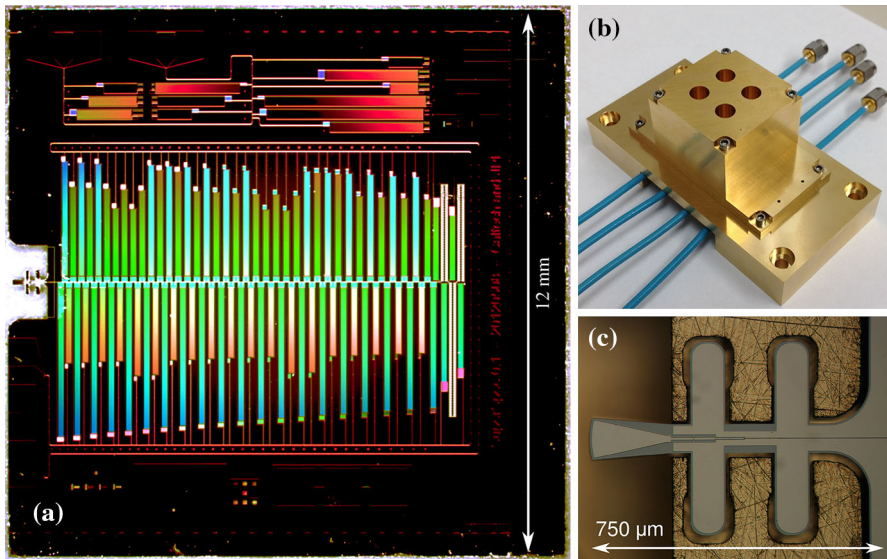
Fig. 2 **a** Prototype SuperSpec die; mm-wave feedline runs from *left* to *right* along the center past an array filter channels. A second array of dark test devices is located at the *top* of the die. **b** Four channel prototype horn block and test package. **c** Wide-bandwidth mm-wave probe mounted in the horn waveguide (Color figure online)

to couple to a waveguide probe fabricated on the 25 μm thick device layer of the SOI wafer which supports the spectrometer chip. The radial stub probe transitions through a CPW transmission line to form the broadband impedance match between the waveguide and the microstrip of the spectrometer. By careful design of the ground plane of the waveguide probe, coupling to higher order modes in the probe channel is suppressed without the need for wire bonds or beam-leads [12]. Simulation of this design show a coupling efficiency above 90 % from 190 to 310 GHz. A low pass capacitive metal-mesh filter is placed directly above horn to block harmonics.

3 Measured Performance

The prototype filter was tested in an optical cryostat cooled by a commercial pulse tube cooler (PTC) and a ^{3}He sorption refrigerator with a base temperature of 225 mK. The prototype horn block shown in Fig. 2 looks into the room through a 4K cold aperture, three metal-mesh low pass filters, a quartz IR blocker with low-density polyethylene (LDPE) anti-reflection coatings, and a 70 mm clear aperture high-density polyethylene (HDPE) window.

In cold tests of several devices from the most recent optical wafer, the median yield for operable KID resonators is 78 out of the 81 expected optical devices, with no critical flaws that disable an entire array. Values of the coupling quality factor (Q_c) are consistently close to the design value of 2×10^5, while the internal quality factor (Q_i) is $\geq 10^6$. The total quality factor, $Q_r = 1/(1/Q_i + 1/Q_c)$, is shown for a typical device in Fig. 3.
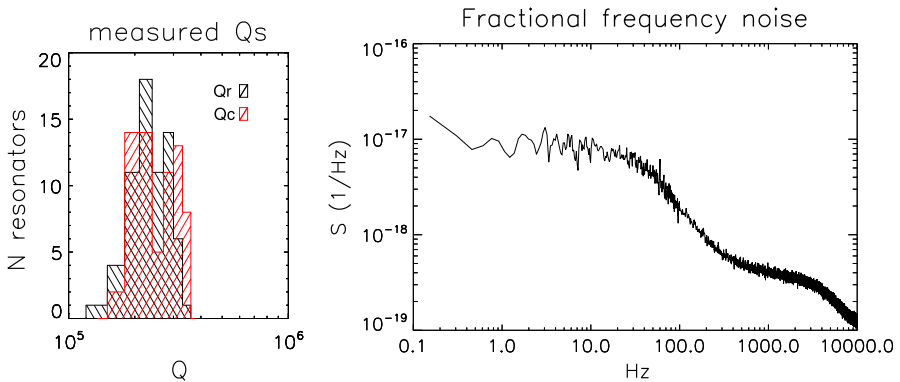
Fig. 3 (*Left*) measured readout Q values for one SuperSpec array. (*Right*) measured fractional frequency noise for a recent single SuperSpec detector under conditions specified in the text (Color figure online)

The responsivity of SuperSpec channels was inferred using beam-filling absorber placed outside the cryostat window at a temperature of either 300 or 77 K, in conjunction with the measured channel profiles. When Q_{loss} is small, the total optical power on an isolated, filter-coupled detector at frequency F_{mm} with matched mm-wave Qs will be approximately $P_{opt} = \eta k \Delta T F_{mm}/2\mathscr{R}$, where η includes an estimated 70 % transmission through the optical filter stack and 50 % power loss to beam truncation at 4 K inside the cryostat, and we have assumed a single-moded, single-polarization horn. For a detector with $R \sim 300$ and $F_{mm} = 250$ we expect a 0.45 pW difference in loading.

The most responsive $\mathscr{R} \sim 300$ channels tested exhibit a fractional frequency shift of $\Delta F/F = 10^{-5}$, corresponding to an estimated responsivity-volume product $RV = 8 \times 10^8 \mu m^3 W^{-1}$, under a constant load of 7×10^{-4} pWμm^{-3}. These values do not include the effect of dissipating power in only a portion of the inductor volume, which increases the inferred response by at most a factor of two.

This inferred responsivity is much lower than predicted from Mattis-Bardeen relations, even assuming recently reported electron density of states, $N_0 = 4 \times 10^{10} eV^{-1} \mu m^{-3}$ [13,14]. It is also low compared to scaled measurements of the MAKO 350 μm camera pixels which are made from similar TiN films from the same facility [15]. We are currently investigating the source of this discrepancy. Significant problems with mm-wave coupling simulations seems unlikely for two reasons. First, measured $\mathscr{R}$ values of the widest filtered channels are close to design values. Second, the 10 dB drop in total power measured over the instrumented segment of the terminator agrees with simulations to within the uncertainty associated with our optical band.

Typical SuperSpec resonators from the most recent wafer show measured fractional frequency noise at the level of $1–2 \times 10^{-17} Hz^{-1}$ at a demodulated frequency of 1 Hz when operated 3 dB below bifurcation (-130 dBm at device input), at a stage temperature of 250 mK. A typical noise power spectral density (PSD) plot is shown in Fig. 3. The plateau at 1 kHz is first stage amplifier noise with an analog low-pass filter roll-off. The noise below 100 Hz is present only in the frequency direction of resonators. Readout power and temperature scaling suggest TLS noise is dominant,

despite the shallower than $f^{-1/2}$ frequency dependence. More detailed characterization is currently underway.

4 Refined Second Generation Design

Using measured values for fractional frequency noise (S_{ffr}, the PSD in units of Hz^{-1}) and apparent responsivity (frequency shift in Hz/W) of the SuperSpec devices, we estimate an noise equivalent power (NEP) referenced at the detector of $\text{NEP} = \sqrt{S_{\text{ffr}}}/R = 3 \times 10^{-16}\,\text{WHz}^{-1/2}$. This is significantly higher than the background limit for proposed science applications, and is due primarily to the low measured responsivity. We are currently pursuing two programs designed to improve this NEP.

The first is a systematic exploration of possible contributions to the low inferred responsivity, including independent checks on the horn and mm-wave probe transmission and the responsivity of TiN direct absorption camera pixels to radiation in our observing band. The second is a test chip redesign which includes both new diagnostic features and devices which have been modified to improve responsivity, decrease TLS noise, and increase resilience to fabrication variation (see Fig. 1c). The first test dies with the new design are in fabrication.

References

1. E. Shirokoff et al., Proc. SPIE **8452**, 84520R (2012)
2. P.S. Barry et al., Proc. SPIE **8452**, 84522F (2012)
3. A. Kovács et al., Proc. SPIE **8452**, 84522G (2012)
4. J.A. Tauber, N.R. Erickson, Rev. Sci. Inst. **62**, 1288 (1991)
5. C.J. Galbraith et al., IEEE Trans. Circ. Syst. I **55**, 969 (2008)
6. C.J. Galbraith, Ph.D. thesis, U. Michigan (2008)
7. A. Endo et al., J. Low Temp. Phys. **167**, 341 (2012)
8. A. Endo et al., Appl. Phys. Lett. **103**, 032601 (2013)
9. H.G. Leduc et al., Appl. Phys. Lett. **97**, 102509 (2010)
10. S. Doyle et al., JLTP **151**, 530 (2008)
11. J. Leech et al., A&A **532**, A61 (2011)
12. J.W. Kooi et al., in *Fourteenth International Symposium on Space Terahertz Technology*, ed. by C. Walker, J. Payne, 2003, p. 127
13. J. Zmuidzinas, Ann. Rev. Cond. Matter Phys. **3**, 169 (2012)
14. J. Gao et al., Appl. Phys. Lett. **101**, 142602 (2012)
15. C.M. McKenney et al., Proc. SPIE **8452**, 84520R (2012)